PREDICTING INHOMOGENEOUS MIXING USING PDF METHODS: RESOLVING MIXING AND EVAPORATION IN THE SMALLEST CLOUD FILAMENTS

Christopher A. Jeffery *
Space and Remote Sensing Sciences (ISR-2), LANL, Los Alamos, NM
Jon M. Reisner
Atmospheric, Climate and Environmental Dynamics (EES-2), LANL, Los Alamos, NM

1. INTRODUCTION

Early convective cloud parameterizations assumed that cloud interiors were well mixed—the so-called "homogeneous mixing" approximation (Jonas and Mason 1982). This assumption was challenged by Baker et al. (1980) who first pointed out that the actual mixing of two fluid elements with different relative humidity, RH, occurs via diffusion across narrow centimeter-scale filaments with advection controlling the contact rate of unmixed fluid elements. The converse of this statement—fluids remain unmixed in the absence of diffusion—is a consequence of the well-known phase preservation property of Louiville equations.

Based on this phenomenological picture, Baker et al. proposed that turbulent mixing in clouds is either "inhomogeneous" or "extreme inhomogeneous" in nature as illustrated in Fig. 1. During inhomogeneous mixing [Fig. 1b)] cloud droplets experience a range of subsaturations in filaments with different ratios of cloud/environmental air. The net result is a broadening of the size-spectrum to smaller sizes. In contrast, during extreme inhomogeneous mixing [Fig. 1c)] some fraction of droplets completely evaporate in subsaturated filaments and thereby restore RH to unity—the size of the remaining droplets are unchanged but the number concentration decreases.

In this work, we consider the isobaric evolution of clear and cloudy air during turbulent mixing in the absence of secondary nucleation and we study the broadening of the droplet size spectrum to smaller sizes due to evaporation. Baker et al. introduced three characteristic time scales: an entrainment time, the time for molecular diffusion across filaments and the evaporation time for a single droplet. For the present scenario, we demonstrate that the nature of mixing [e.g. homogeneous vs inhomogeneous] is primarily determined by

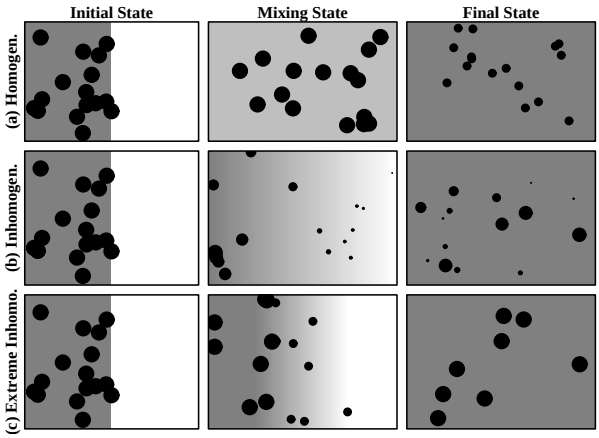

Figure 1: Schematic of different mixing scenarios: (a) Homogeneous, (b) Inhomogeneous and (c) Extreme Inhomogeneous.

the Damköhler number (Damköhler 1940):

$$\mathrm{Da} \equiv \mathrm{t_{eddy}}/\mathrm{t_{react}},$$

the ratio of turbulent ($\mathrm{t_{eddy}}$) and reactive ($\mathrm{t_{react}}$) time scales, where—for cloud evaporation—$\mathrm{t_{react}}$ is given by the characteristic time for phase change (Squires 1952) such that

$$\mathrm{Da} = 4\pi N D_v \mathrm{t_{eddy}} \left\langle r^2/(r+a) \right\rangle_{t=0} \qquad (1)$$

where N is the initial droplet number density in the cloudy air, D_v is the diffusivity of water vapor, r is droplet radius, $a = 2\ \mu\mathrm{m}$ is an accommodation length, and $\langle\cdot\rangle_{t=0}$ is an ensemble average at time zero. For the present mixing scenario and typical model grid sizes and atmospheric conditions, Da spans four orders of magnitude in the range 10^{-2} to 10^{2} as discussed in Jeffery and Reisner (2006).

Evaluation of the impact of Da on the evolution of RH is complicated by the non-linear nature of mixing and evaporation. Moment formulations suffer from the well-known closure problem that information about statistical moments of every order is needed to have closed

*Corresponding author address: Christopher A. Jeffery, Los Alamos National Laboratory (ISR-2), PO Box 1663, Mail Stop D-436, Los Alamos, NM 87545, USA. Tel.: (505) 665-9169; fax: (505) 664-0362. Email: cjeffery@lanl.gov

non-linear terms. Probability density function (PDF) methods offer a distinct advantage over moment approaches since non-linear reaction terms like evaporation are more easily evaluated. The PDF equation for advection-diffusion requires evaluation of the conditional Laplacian. However, evaluation of this statistic using a Gaussian mixing assumption leads to unphysical behavior in the evolution of the scalar PDF unless the PDF is strictly Gaussian itself.

In this study we use a technique called "mapping closure" (Chen et al. 1989) to evaluate the conditional Laplacian, that does not suffer from the deficiencies of a purely Gaussian closure. The PDF-equation for RH is introduced in Sec. 2 and Chen et al.'s mapping closure is briefly summarized. In Sec. 3 we introduce a droplet number mixing model for the conditional evaluation of N, and Sec. 4 summarizes the impact of Da on the evolution of RH and the droplet size distribution, $f(r)$. Sec. 5 discusses total droplet evaporation during mixing and Sec. 6 contains a brief summary.

2. PDF-EQUATION FOR RH

In analogy with the well-known equation for $f(r)$, the equation for the RH-PDF is given by:

$$\frac{\partial \mathcal{P}(\mathrm{RH})}{\partial t} = -\frac{\partial}{\partial \mathrm{RH}}\left[\left\langle \frac{\partial \widetilde{\mathrm{RH}}}{\partial t}\middle|\, \widetilde{\mathrm{RH}} = \mathrm{RH}\right\rangle \mathcal{P}(\mathrm{RH})\right] \tag{2}$$

where $\mathcal{P}(\mathrm{RH})d\mathrm{RH}$ is the probability that RH is in the range $[\mathrm{RH}, \mathrm{RH}+d\mathrm{RH}]$, $\widetilde{\mathrm{RH}}(\boldsymbol{x},t)$ is the RH field and $\langle \partial\widetilde{\mathrm{RH}}/\partial t|\widetilde{\mathrm{RH}} = \mathrm{RH}\rangle$ is the conditional derivate of $\widetilde{\mathrm{RH}}$ evaluated on level sets of RH.

For temperature differences between the cloud/environmental air that are small compared to the Clausius-Clapeyron temperature* $R_v T^2/L_v$ and assuming equality of the diffusivities of water vapor and temperature, $\widetilde{\mathrm{RH}}$ obeys the usual advection–diffusion equation with an evaporative source term. Substitution of the diffusive contribution to the conditional derivative of $\widetilde{\mathrm{RH}}$ gives the conditional Laplacian describing the impact of diffusion on $\mathcal{P}(\mathrm{RH})$:

$$D_* \left\langle \nabla^2 \widetilde{\mathrm{RH}}\middle|\, \widetilde{\mathrm{RH}} = \mathrm{RH}\right\rangle \tag{3}$$

where D_* is the vapor/temperature diffusivity.

2a. *Evaluation of conditional advection-diffusion*

Evaluation of Eq. (3) is the fundamental closure problem in the evaluation of PDFs describing advection-diffusion systems. Gaussian closure results in an advection equation for the PDF that does not give the expected relaxation toward Gaussian statistics unless the PDF is strictly Gaussian itself. Chen et al. (1989) proposed a technique called mapping closure to evaluate Eq. (3) that exhibits realistic relaxation for strongly non-Gaussian PDFs and will be used in the present study. In this new approach, illustrated in Fig. 2, a time-dependent non-Gaussian PDF is mapped to a time-independent Gaussian random field. Once the mapping is established, the map can be evolved in time without approximation since the statistics of the Gaussian random field are known.

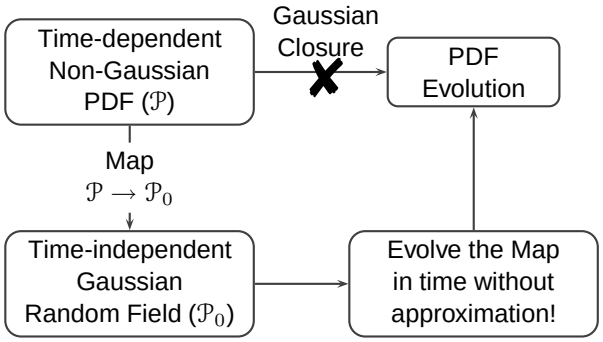

Figure 2: Schematic of mapping closure.

Once the time-dependent mapping $\mathrm{RH} = X(\mathrm{RH}_0, t)$ is established, $\mathcal{P}$ is given by

$$\mathcal{P}(\widetilde{\mathrm{RH}} = \mathrm{RH}, t) = \mathcal{P}_0(\widetilde{\mathrm{RH}_0} = \mathrm{RH}_0)\left(\partial X/\partial \mathrm{RH}_0\right)^{-1}, \tag{4}$$

where $\mathcal{P}_0$ denotes the single-point PDF of the centered Gaussian random field. Closure is achieved by assuming that the (unknown) spatial statistics of $\widetilde{\mathrm{RH}}$ are the same as the surrogate field $\widetilde{\mathrm{RH}_0}$. In particular, this implies

$$\langle \nabla^2 \widetilde{\mathrm{RH}} | \mathrm{RH}\rangle = \langle \nabla^2 \widetilde{\mathrm{RH}_0} | X(\mathrm{RH}_0)\rangle.$$

Using this approach, the evolution equation for X is an explicit function of the spatial statistics of the surrogate field. Chen et al. derive

$$\frac{\partial X}{\partial t} = \chi_0 \left(-\frac{\mathrm{RH}_0}{\langle \widetilde{\mathrm{RH}_0^2}\rangle}\frac{\partial X}{\partial \mathrm{RH}_0} + \frac{\partial^2 X}{\partial \mathrm{RH}_0^2}\right) + Q(X), \tag{5}$$

where $\chi_0 \equiv \kappa\langle |\boldsymbol{\nabla}\widetilde{\mathrm{RH}_0}|^2\rangle$ and $Q(\widetilde{\mathrm{RH}})$ is the microphysical source term in the advection-diffusion equation for RH. The final step in the derivation relates χ and χ_0, using either Gaussian relations (Chen et al. 1989) or direct evaluation of $\langle X^2\rangle$ in (5):

$$\chi = \chi_0 \left\langle \left(\partial X/\partial \mathrm{RH}_0\right)^2 \right\rangle.$$

*T is temperature, R_v is the water vapor gas constant and L_v is the latent heat of vaporization.

Note that a complete closure requires independent specification of χ which we discuss in Sec. 2b.

Eq. (5) reveals the essential physics of X evolution. The first term on the rhs of (5) advects X away from $\mathrm{RH}_0 = 0$ toward both $+\infty$ and $-\infty$. In addition, diffusion smooths the features of X leading to near-Gaussian statistics via Eq. (5). This is the essential feature of mapping closure that assures physically reasonable behavior: anti-diffusional behavior in RH-space is translated into diffusional evolution in RH_0-space that is stable and mathematically well-defined. As shown by Gao (1991a,b), this RH_0-space evolution leads to a well-mixed state that is near-Gaussian but retains some memory of its initial non-Gaussian form, in good agreement with numerical experiment.[†]

2b. *Specification of* χ

PDF methods, including mapping closure, require independent specification of the scalar dissipation rate $\chi(t)$. Here we use a simple Newtonian damping term

$$\chi(t) = \mathrm{var}(\mathrm{RH})/\mathrm{t}_{\mathrm{eddy}}, \tag{6}$$

where a time-independent $\mathrm{t}_{\mathrm{eddy}}$ is specified a priori. Specification of a linear dependence of χ on $\mathrm{var}(\mathrm{RH})$ is frequently employed in cloud modeling studies and dates back to the early work of Mellor and Yamada (1974) and Wyngaard and Coté (1974), among others.

3. DROPLET MIXING MODEL

Equating the conditional derivative in Eq. (2) to the sum of diffusive and evaporative contributions and introducing the non-dimensional time scale $\tau = t/\mathrm{t}_{\mathrm{eddy}}$ gives

$$\begin{aligned} \partial\mathcal{P}/\partial\tau &= -(\partial/\partial\mathrm{RH})\left[D_*\mathrm{t}_{\mathrm{eddy}}\left\langle\widetilde{\nabla^2\mathrm{RH}}\right\rangle_\tau\mathcal{P}\right] \\ &\quad + \mathrm{Da}\frac{\partial}{\partial\mathrm{RH}}\left[\frac{\langle N|\mathrm{RH}\rangle_\tau}{N}(\mathrm{RH}-1)\mathcal{P}\right] \end{aligned} \tag{7}$$

where we have assumed that mean droplet radius changes little during a mixing event. The advantage of the constant radius limit is that it leads to mixing and evolution that are independent of the specifics of the droplet size distribution. Note that $\langle\widetilde{\nabla^2\mathrm{RH}}\rangle_\tau$ is evaluated using mapping closure in what follows.

The terms in square brackets in Eq. (7) are of order unity. Thus the Damköhler number, Da, determines the relative strengths of the evaporative and advective-diffusive contributions to the RH-PDF evolution as expected.

[†]Additional information on mapping closure including simulations and comparisons with other Gaussian closures can be found at LANL, cited (2006).

In order to model $\langle N|\mathrm{RH}\rangle_\tau$ we must first specify the present mixing scenario. We consider the mixing of equal volumes of clear and cloudy air with $\mathrm{RH} = \mathrm{RH}_{\mathrm{env}}$ in the clear volume and $\mathrm{RH} = 1$ in the cloudy volume. Formally, $\mathcal{P}_{\tau=0} = 0.5\delta(\mathrm{RH}-\mathrm{RH}_{\mathrm{env}}) + 0.5\delta(\mathrm{RH}-1)$. The final state is $\mathcal{P}_{\tau\to\infty} = \delta(\mathrm{RH}-1)$. We introduce a droplet number mixing model for $\langle N|\mathrm{RH}\rangle_\tau$ based on the following considerations. In the limit that droplet and RH trajectories coincide and in the absence of evaporation, $\langle N|\mathrm{RH}\rangle_\tau$ is proportional to the relative volume fractions of clear and cloudy air:

$$\langle N|\mathrm{RH}\rangle_\tau/N = (\mathrm{RH}(\tau)-\mathrm{RH}_{\mathrm{env}})/(1-\mathrm{RH}_{\mathrm{env}}).$$

Evaporation must necessarily modify this relation; as droplets evaporate and local RH increases, the relative fraction of drops becomes less than this volume fraction relation indicates. We consider an analytic parameterization of $\langle N|\mathrm{RH}\rangle_\tau$ of the form

$$\langle N|\mathrm{RH}\rangle_\tau = F(t)N\left(\frac{\mathrm{RH}-\mathrm{RH}_{\mathrm{env}}}{1-\mathrm{RH}_{\mathrm{env}}}\right)^\beta, \tag{8}$$

for $\mathrm{RH}_{\mathrm{env}} \le \mathrm{RH} \le 1$ where $F(t)$ satisfies the normalization $\int\mathcal{P}(\mathrm{RH})\mathrm{RH}\;\langle N|\mathrm{RH}\rangle = \langle N\rangle$. Eq. (8) states that *on average* the expected droplet concentration increases with increasing RH.

The exponent β in Eq. (8) controls the relative rate at which droplets "mix" into subsaturated regions of largely unmixed environmental air. In particular the limit $\beta\to\infty$ implies infinitely slow droplet mixing while $\beta\to 0$ implies infinitely quick mixing. The value $\beta = 1$ is an exact result for the given initial conditions in the absence of condensation-evaporation, sedimentation and diffusive effects. In Jeffery and Reisner (2006) we derive the expression

$$\beta = 1 + 0.015\mathrm{Da}^{1/2}, \tag{9}$$

which produces evaporation times that are consistent with eddy-diffusive mixing.

4. PDF EVOLUTION

The evolution of the PDF of RH is shown in Fig. 3 for $\mathrm{Da} = 100$ and $\mathrm{RH}_{\mathrm{env}} = 0.6$. At large Damköhler number, the predictions of the present approach are consistent with the phenomenological model of Baker et al.. The relatively low probability of finding RH in the range $0.62 < \mathrm{RH} < 0.98$ illustrates that mixing of fluid elements is confined to narrow filaments with small volume fraction. Restoration of RH to unity in filaments due to evaporation occurs at a faster rate than the diffusive growth of the filament—this is the fundamental nature of hydrodynamic reaction at high Da.

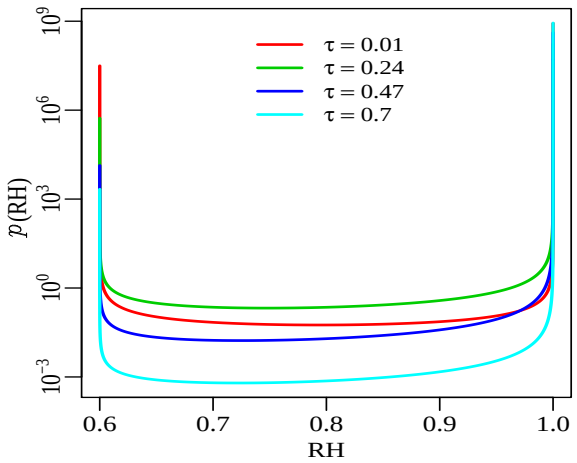

Figure 3: Evolution of $\mathcal{P}(\mathrm{RH})$ calculated from Eq. (7) with $\mathrm{Da} = 100$ and $\mathrm{RH}_{\mathrm{env}} = 0.6$.

A comparison of the cumulative distribution function (CDF) that $\mathrm{RH} \leq 0.99$ for $\mathrm{Da} \in [10, 1000]$ is shown in Fig. 4. The top figure shows $\mathrm{CDF}(\mathrm{RH} \leq 0.99)$ while the bottom figure depicts the CDF weighted by droplet number as modeled by Eq. (8). The results illustrated in Fig. 4 re-emphasize the fundamental connection between Damköhler number and Baker et al.'s concept of inhomogeneous mixing. Specifically, Fig. 4 demonstrates that the relative fraction of droplets that experience a subsaturated environment decreases with increasing Da.

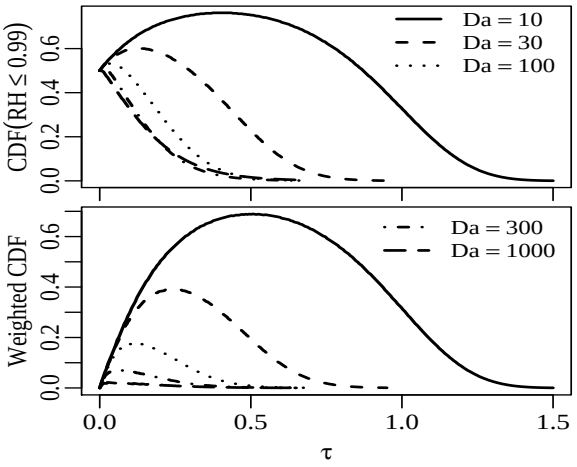

Figure 4: Cumulative probability $\mathrm{RH} \leq 0.99$ (top) and CDF weighted by $N(\mathrm{RH})/N$ (bottom).

Determination of the droplet size spectrum, $f(r)$, requires Lagrangian information of the supersaturation along droplet trajectories. Let

$$(\mathrm{S_{int}})_A = \frac{1}{\tau(1-\mathrm{RH_{env}})}\int_0^\infty dt\ \mathrm{RH}_A(t) - 1$$

be the normalized supersaturation integral of the droplet labeled "A" such that $\mathrm{RH}_A(t)$ is the local supersaturation experienced by A at time t. The present approach provides $N(\mathrm{RH})$ but not $\mathrm{S_{int}}$ without further assumption. We introduce a Lagrangian droplet evolution model in RH-space in which droplets randomly move to a new RH-bin after at time $\mathrm{t_{clock}}$ which is exponentially distributed with mean $\mathrm{t_{eddy}}$. Thus the Lagrangian mixing process is modeled with a renewal process with exponential distributed mixing times.

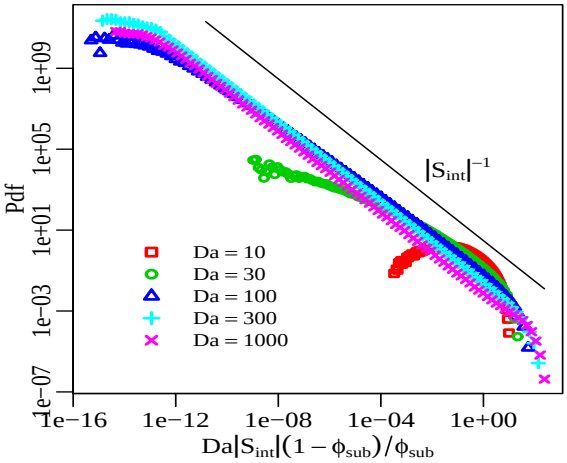

Figure 5: PDF of $\mathrm{Da}|\mathrm{S_{int}}|$ for $\mathrm{Da} \in [10, 1000]$.

The PDF of $|\mathrm{S_{int}}|$ calculated using Eq. (7) and a renewal process for Lagrangian droplet trajectories in RH-space is shown in Fig. 5. Note that $\langle \mathrm{Da}|\mathrm{S_{int}}|(1-\phi_{\mathrm{sub}})/\phi_{\mathrm{sub}}\rangle = 1$ where ϕ_{sub} is the volume fraction of subsaturated (entrained) air. The figure reveals that most droplets do not experience significant subsaturation during mixing at large Da while for smaller Da most droplets experience a subsaturation that is greater than the minimum.

The asymptotic behavior $\mathcal{P}(|\mathrm{S_{int}}|) \sim |\mathrm{S_{int}}|^{-1}$ at large Da is a seminal feature of the Gaussian mixing assumptions inherent in mapping closure. This can be derived from solutions of the map X but it is more readily apparent from the Gaussian model with microphysical source term

$$\frac{\mathcal{P}(\mathrm{RH})}{\partial t} = -\frac{\partial}{\partial \mathrm{RH}}\left[\frac{\mathrm{RH} - \langle \mathrm{RH}\rangle}{\mathrm{t_{eddy}}}\mathcal{P}\right]$$

which, upon transforming to $|\mathrm{S_{int}}|$ and using $\langle|\mathrm{S_{int}}|\rangle \approx 0$ gives the steady-state solution $\mathcal{P}(|\mathrm{S_{int}}|) \sim |\mathrm{S_{int}}|^{-1}$.

The effect of our new PDF model of mixing on the droplet size spectrum is shown in Fig. 6 and calculated such that 15% of droplets completely evaporate during the mixing process. The figure reveals that decreasing Da broadens the droplet spectrum to smaller sizes.

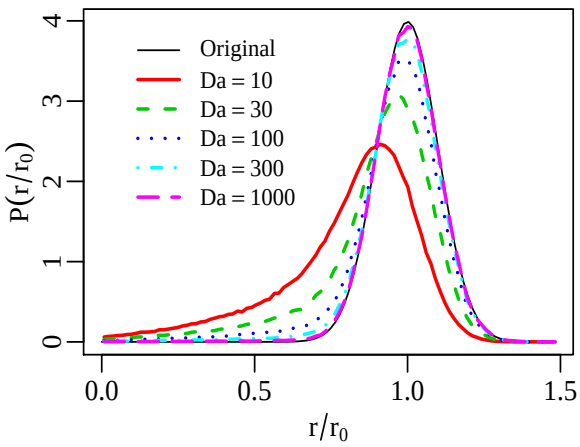

Figure 6: Droplet spectra assuming a Gaussian initial state with $\sigma = 0.1 r_0$.

5. DROPLET EVAPORATION

The dependence of total droplet evaporation on Damköhler number is illustrated in Fig. 7. Here, N_i is the initial **grid-cell averaged** droplet number concentration, N_f is the final concentration after mixing, and $(\rho_l)_i$ and $(\rho_l)_f$ are the initial and final liquid water densities, respectively. The point $(0.5, 0.5)$ refers to a 50% change in cloud liquid water density during mixing with no change in droplet size and complete evaporation of half the drops. The figure reveals that increasing Da and decreasing ϕ_{sub} increases the number of droplets that evaporate completely.

The results of Fig. 7 are summarized in Fig. 8 for $(\rho_l)_f/(\rho_l)_i = 0.85$. Here what is plotted is the statistic

$$\beta = \frac{N_f/N_i - (\rho_l)_f/(\rho_l)_i}{1 - (\rho_l)_f/(\rho_l)_i}$$

such that $\beta = 1$ for completely homogeneous mixing ($N_f = N_i$) and $\beta = 0$ for extreme inhomogeneous mixing ($N_f/N_i = (\rho_l)_f/(\rho_l)_i$). The figure reveals that the nature of mixing depends logarithmically on Da for $\phi_{\mathrm{sub}} > 0.2$ but a strong dependence on Da is seen for $\phi_{\mathrm{sub}} < 0.2$.

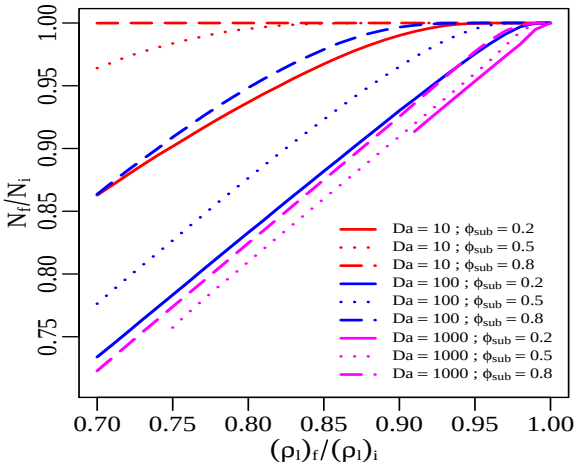

Figure 7: Dependence of droplet evaporation on Da.

6. SUMMARY

In this work the PDF equation for RH has been derived and closed using (i) mapping closure to evaluate the conditional Laplacian and (ii) a droplet number mixing model to evaluate $\langle N|\widetilde{\mathrm{RH}} = \mathrm{RH}\rangle$. The central conclusions of this study are summarized in Fig. 9. The concepts of "inhomogeneous mixing" and "extreme inhomogeneous mixing" introduced by Baker et al. are shown to be equivalent to hydrodynamic reaction at $\mathrm{Da} = \mathcal{O}(1)$ and large Da, respectively. For the present mixing scenario and typical atmospheric conditions "homogeneous mixing" does not occur. In addition, due to the dependence of Da on N indicated by Eq. (1), we find that increasing N increases Da which thereby decreases the dispersion of the droplet size spectrum to smaller scales and increases total droplet evaporation.

A seminal feature of the present approach is the asymptotic behavior $\mathcal{P}(|\mathrm{S_{int}}|) \sim |\mathrm{S_{int}}|^{-1}$ at large Da which is a result of the Gaussian assumption inherent in mapping closure. This feature of our new PDF model of mixing requires observational validation.

REFERENCES

Baker, M. B., R. G. Corbin, and J. Latham, 1980: The influence of entrainment on the evolution of cloud droplet spectra: I. A model of inhomogeneous mixing. *Quart. J. Roy. Meteor. Soc.*, **106**, 581–599.

Chen, H., S. Chen, and R. H. Kraichnan, 1989: Prob-

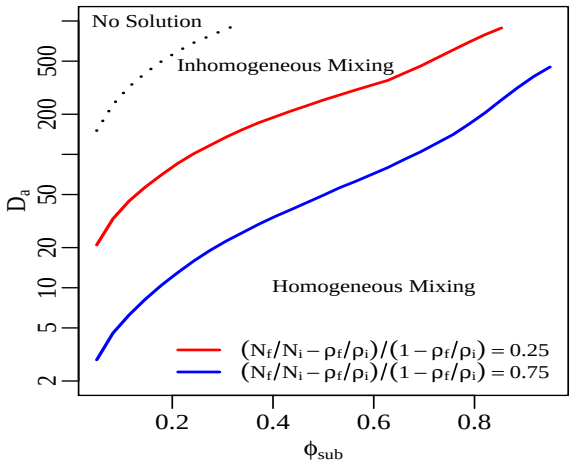

Figure 8: Dependence on the nature of mixing, i.e. homogeneous vs inhomogeneous, on Da and ϕ_{sub} for $(\rho_l)_f/(\rho_l)_i = 0.85$.

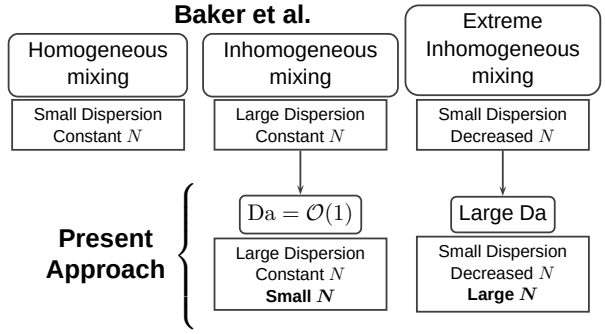

Figure 9: Schematic of present results.

ability distribution of a stochastically advected scalar field. *Phys. Rev. Lett.*, **63**, 2657–2660.

Damköhler, G. Z., 1940: Influence of turbulence on flame velocity in gaseous mixtures. *ZH Electrochem*, **46**, 601.

Gao, F., 1991a: An analytical solution for the scalar probability density function in homogeneous turbulence. *Phys. Fluids*, **A3**, 511–513.

— 1991b: Mapping closure and non-gaussianity of the scalar probability density functions in isotropic turbulence. *Phys. Fluids*, **A3**, 2438–2444.

Jeffery, C. A. and J. M. Reisner, 2006: A study of cloud mixing and evolution using PDF methods. 1. Cloud front propagation and evaporation. *J. Atmos. Sci.*, in press.

Jonas, P. R. and B. J. Mason, 1982: Entrainment and the droplet spectrum in cumulus clouds. *Quart. J. Roy. Meteor. Soc.*, **108**, 857–869.

LANL, cited, 2006: Statistical cloud physics web page, [`http://aerosols.lanl.gov/~cjeffery`.].

Mellor, G. L. and T. Yamada, 1974: A hierarchy of turbulence closure models for planetary boundary layers. *J. Atmos. Sci.*, **31**, 1791–1806.

Squires, P., 1952: The growth of cloud drops by condensation. 1. General characteristics. *Aust. J. Sci. Res.*, **A5**, 59–86.

Wyngaard, J. C. and O. R. Coté, 1974: The evolution of a convective planetary boundary-layer— a higher-order-closure model study. *Bound.-Layer Meteor.*, **7**, 289–308.